Reaction Chemistry & Engineering

On-the-Spot Quenching for Effective Implementation of Cooling Crystallization in Continuous-Flow Microfluidic Device

Journal:	*Reaction Chemistry & Engineering*
Manuscript ID	RE-ART-01-2022-000029
Article Type:	Paper
Date Submitted by the Author:	26-Jan-2022

Complete List of Authors:	Coliaie, Paria; University of Illinois at Chicago, Department of Chemical Engineering Kelkar, Manish; AbbVie Inc, Process R&D Korde, Akshay; AbbVie Inc, Langston, Marianne; Takeda Pharmaceuticals USA Inc Lexington, Pharmaceutics Research - Analytical Development Liu, Chengxiang; Biogen Inc, Pharmaceutical Development Nazemifard, Neda; Takeda Pharmaceuticals USA Inc Lexington, Chemical Process Development Patience, Daniel; Biogen Inc, Chemical Process Development Skliar, Dimitri; Bristol-Myers Squibb Co Research & Development, Chemical and Synthetic Development Nandkishor, Nere; AbbVie Inc, Process R&D Singh, Meenesh; University of Illinois at Chicago, Chemical Engineering

On-the-Spot Quenching for Effective Implementation of Cooling Crystallization in Continuous-Flow Microfluidic Device

Paria Coliaie[1], Manish S. Kelkar[2], Akshay Korde[2], Marianne Langston[3], Chengxiang Liu[4], Neda Nazemifard[5], Daniel Patience[4], Dimitri Skliar[6], Nandkishor K. Nere[1,2], and Meenesh R. Singh[1,*]

[1]Department of Chemical Engineering, University of Illinois at Chicago, Chicago, IL 60607

[2]Center of Excellence for Isolation & Separation Technologies (CoExIST), Process R&D, AbbVie Inc., North Chicago, IL 60064

[3]Pharmaceutics Research – Analytical Development, Takeda Pharmaceuticals International Co., Cambridge, MA 02139

[4]Pharmaceutical Development, Biogen, Cambridge, MA 02142

[5]Chemical Process Development, Takeda Pharmaceuticals International Co., Cambridge, MA 02139

[6]Chemical Process Development, Product Development, Bristol Myers Squibb Co., New Brunswick, NJ 08901

Corresponding Author:

Prof. Meenesh R. Singh
Assistant Professor
Department of Chemical Engineering
929 W. Taylor St.
University of Illinois at Chicago
Chicago, IL 60607
Tel: (312) 996-3424
Email: mrsingh@uic.edu

Keywords: Continuous Crystallization, Cooling Crystallization, Polymorph Screening, Growth Rates, Continuous-Flow Microfluidics

Abstract

Cooling crystallization is a well-established separation technique in pharmaceutical, agrochemical, and wastewater treatment processes where dissolved species need to be removed selectively from a solution without adding any external agents. Effective implementation of cooling crystallization in microfluidic devices has the potential to bring transformative impact in the screening of crystalline materials. A primary challenge has been the existence of large temperature gradients near the entrance of the microfluidic channel that causes variations in supersaturation. Additionally, the depletion of supersaturation due to nucleation and growth of crystals leads to variation in the downstream composition. The morphology, polymorph, and growth rate data obtained in such varying conditions may not be adequate for scale-up. So far, no continuous-flow microfluidic device has been reported for studying the cooling crystallization under controlled conditions. Here, we implement and evaluate on-the-spot quenching strategies in a continuous-flow microfluidic device that reduces temperature gradients for homogeneous supersaturation and allows trapping of crystals for in-situ measurement of the morphology, percentage polymorphs, and growth rates. The first strategy involves a collar of the cooling jacket around the micromixer, and the second strategy utilizes the mixing of saturated hot and cold solutions. The efficacy of these strategies is evaluated experimentally and computationally. The cooling jacket strategy is better suited to study higher supersaturations, and the hot-and-cold-mixing strategy is preferred for targeting the lower range of supersaturations. Both cooling strategies are effective in measuring the growth rates of L-glutamic acid crystals at given supersaturations and temperatures. These strategies also show a similar trend in the decrease of β-form of L-glutamic acid crystals with increasing supersaturation. These on-the-spot quenching strategies can be implemented to a wide range of continuous-flow microfluidic devices for various applications.

1. Introduction

Cooling crystallization is a preferred separation technique in pharmaceutical, agrochemical, and wastewater treatment processes where dissolved species need to be removed selectively from a solution without adding any external agents such as antisolvents, additives, pH, modulators, etc.[1] It can be implemented effectively if the solute has a significant solubility difference with respect to temperature. The necessary driving force, i.e., supersaturation, for the cooling crystallization is created by reducing the temperature of the solution towards a state of lower solubility. For such a crystallization process, it is essential to maintain a homogenous temperature of the solution and minimize the temperature gradients that are dominant around the entrance of flow crystallizers and around the walls of the batch crystallizers during cooling. Rapid cooling in conventional flow and batch crystallizers is typically achieved by implementing a convection cooling jacket with an external control system.[2] However, such implementations for convective cooling in microfluidics are quite difficult due to space constraints and the miniaturized size of the device.[3] As a result, the continuous-flow microfluidic devices have not been well-utilized to study cooling crystallization. Effective implementation of cooling crystallization in continuous-flow microfluidics devices can help screening of morphology, polymorph, and growth rates at controlled supersaturations.

Different types of cooling strategies have been employed for microtiter and microfluidic systems (see Figure 1). Here the primary purpose of these techniques is to rapidly cool the entering hot solution in the microchannel or the initial hot solution in the microtiter to a lower temperature. One of the most common techniques is thermoelectric cooling using the Peltier device (see Figure 1A).[4] It has been implemented to study nucleation of protein crystals in 400-well plate,[5] screen nucleation kinetics of colloidal crystals,[6] perform rapid PCR-based analysis.[7] The effective thermoelectric cooling requires higher thermal conductance of microfluidic devices. However, most microfluidic devices are made of polymers with lower thermal conductivity. The higher thermal resistance of microfluidic devices and inefficient contact with the Peltier device often leads to entrance effects in continuous-flow microfluidic devices. The other approach for local cooling is to use either endothermic mixing or reaction near the microchannel.[8] Alternatively, phase change materials that transform from liquid to gas phase can be used to cool down the microchannels (see Figure 1B).[9] In such cooling schemes, the reduction in reaction rates due to depletion of reactants in the cooling channels can result in temperature gradients along the microchannels. Alternatively, the coolants with higher specific heat capacities can be used to maintain a uniform temperature. Figure 1C shows a configuration of droplet-based microfluidic setup, which includes a long capillary tube immersed in a circulating cooling bath. In such systems, the droplets flowing in a continuous phase cool down via diffusive heat transfer. The temperature gradient within the capillary wall may result in a larger temperature variation along the tube. Therefore, this type of cooling is mostly applied to study slow nucleating crystals with longer induction time, such as proteins. Another cooling strategy is convective mixing of hot and cold solutions to quench the hot solution. Figure 1D shows the example of convective mixing in a slug-flow tubular crystallizer, where concentrated hot and cold solutions are mixed in at T-junction and then pumped into the channels along with air to form slugs.[10] The achievable temperatures and concentration of the

mixed stream are limited by the temperature and concentration ranges, respectively, of hot and cold solutions.

A comparative analysis of these four cooling strategies to effectively reduce the temperature of inlet solution with minimum gradients is provided in section S1 of the ESI. Although it is possible to reduce temperature gradients under certain conditions (see Table S1 in section S1 of the ESI), the continuous depletion of solute due to nucleation and growth of crystals in the cooled channels results in a continuous variation of supersaturation. Additionally, faster nucleation and growth may also cause clogging of the microchannels. It is possible to vary the temperature along the cooled channels using a gradient generator to maintain constant supersaturation.[11] However, it is difficult to know a priori how much solute will be depleted in the microchannel and the necessary temperature required to offset the drop in supersaturation. Therefore, an effective microfluidic device for cooling crystallization is required to reduce the temperature gradient, maintain constant supersaturation, and prevent clogging. Recent developments of the continuous-flow crystallization in microfluidic devices have enabled effective screening of crystal morphology, polymorph, size, and kinetic data under controlled conditions.[12,13] These microfluidic devices have cylindrical micromixer with tangential inlets of entering solution at the bottom, which creates cyclonic (or rotational) flow to trap nucleated crystals. The cyclonic flow in the micromixer provides uniform mixing and isothermal conditions to achieve constant supersaturations while allowing the steady growth of trapped crystals.

In most microfluidic devices, the channels tend to get clogged due to accumulation of crystals in downstream. To avoid clogging, there is need for a mechanism to separate crystals from the flow. The cyclonic flow allows bigger crystals to be trapped inside the micromixer without interrupting the flow. Moreover, the diameter of the outlet channel is larger than the average diameter of crystals. Therefore, the continuous-flow microfluidic device is designed to prevent clogging of crystals and any interruption of flow unless the whole micromixer gets filled with crystals. Depending on the crystalline system of interest, the time required for micromixer to be completely filled with crystals would be more than 30 minutes, which is long enough for obtaining the kinetics data.

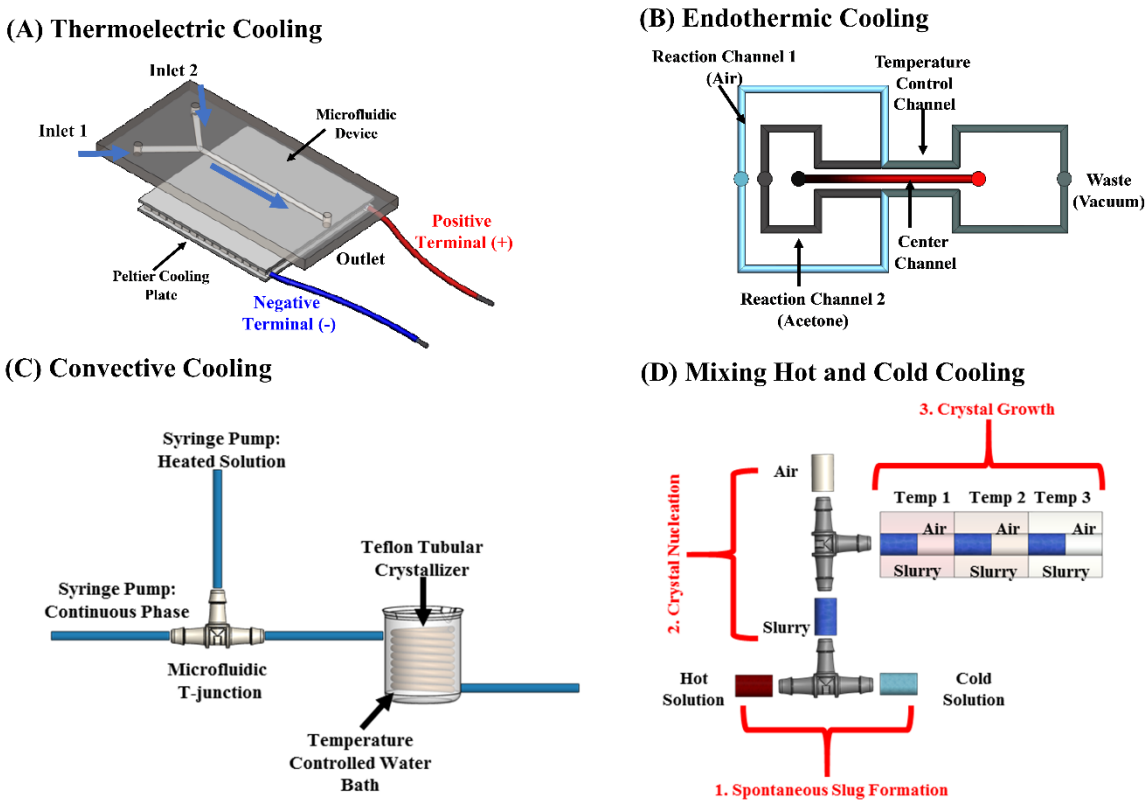

Figure 1: Different types of cooling strategies that has been implemented to study cooling crystallization in microfluidic devices: (A) thermoelectric cooling using Peltier device. The microfluidic device is located on the Peltier device, which is placed on the stage of an optical microscope; (B) endothermic cooling using endothermic reaction or evaporation in cooling channels. The temperature gradient is shown as the red color gradient; (C) convective cooling using external cooling bath; and (D) convective cooling by mixing hot-and-cold streams. (Figures 1B, 1C, and 1D are representative sketches from the referenced studies.[4,9,10])

This study aims at developing effective quenching strategies for these continuous-flow well-mixed microfluidic devices that will enable the screening of crystalline materials through cooling crystallization strategies.[12] Here, two different on-the-spot quenching strategies are introduced that can cool down the inlet solution with minimum possible spatial gradient. The first strategy is inspired by jacketed mixed-suspension mixed-product removal reactors used for batch and semi-batch cooling crystallization in the larger scales. In this design, a cooling jacket is implemented around the lower bottom of the microwell where the inlets are located so that the entering solution is quenched. The cooling jacket has a separate inlet and outlets to recirculate the coolant stream. The second on-the-spot quenching strategy involves the mixing of two separate saturated solutions of higher and lower temperatures. The mixed solution in the microwell attains a lower temperature than the entering hot solution and thereby developing a steady supersaturation. The temperature profile is initially evaluated for both strategies at different flow rates and temperatures of entering solution and coolant and then assessed for the accessible range of supersaturations. The attainable temperature and supersaturation ranges are confirmed both experimentally and computationally.

Finally, the microfluidic devices with and without cooling jackets are 3D printed and then tested to screen the morphology, polymorph, and growth rate of L-glutamic acid crystals grown by cooling crystallization.

2. Theoretical Methods

2.1 Design Consideration to Implement On-the-Spot Quenching Strategies in Multi-Inlet Micromixer Device

The cyclonic flow in the multi-inlet micromixer has been shown to trap crystals effectively in continuous flow conditions.[12] The lower Stokes number (~5.5 x 10^{-3}) in the micromixer allows smaller crystals to flow along the streamlines and disperse uniformly in the solution. However, the near stagnant regions at the bottom and the center of the well allows larger crystals (~300 μm) to settle down at velocities ~2.83 cm s^{-1}.[12] The expected settling velocities for α and β forms of L-glutamic acid are 0.45 cm s^{-1} and 1.6 cm s^{-1}, respectively. These high settling velocities ensures crystals can be trapped, and their growth rate can be measured over time. The details of settling velocity calculations and streamlines of cyclonic flow in micromixer are provided in ESI. Next, we evaluate two distinct quenching strategies to enable on-the-spot cooling in the multi-inlet micromixer device. The first strategy is convective cooling that uses an external cooling jacket, and the second strategy involves convective mixing of a hot and cold solution. While the latter scheme allows on-the-spot quenching of hot and cold solutions to attain equilibrium temperatures, the former scheme requires some additional design considerations to enable on-the-spot quenching. The residence time of solutions in these tiny micromixers (up to 4mm height and 4mm diameter) varies from a few seconds to a few minutes.[13] As the hot solution enters the micromixer from the bottom and rises upward, it will continuously cool down without reaching a steady temperature and thus developing a large temperature variation inside the micromixer. It is nearly impossible to attain equilibrium temperatures in a fully jacketed micromixer with these residence times. Therefore, one of the design considerations is to have a shorter height of cooling jacket not exceeding the diameter of the inlet. The detail for the thermal homogeneity index of bath with longer height is provided in section S3.4 of the ESI. This collar of the cooling jacket ensures that tangentially entering solutions are cooled as they are mixed in a cyclonic flow inside the mixer. The thermal insulation above the collar maintains the temperature of the cooled solution. Figure 2A shows the design of the micromixer with a collar of the cooling jacket. The coolant in the cooling jacket can be set to a sufficiently lower temperature for the entering hot solution to achieve the desired temperature. It depends on the design of the micromixer, thermal and physical properties of coolant, solution, and material of construction, which is discussed in the next section. In this cooling jacket strategy, the temperature and concentration of cooled solution are independent of each other, which allows probing a wider range of supersaturations.

The second cooling strategy does not require any cooling jacket if the insulation of the micromixer is efficient to maintain the temperature of cooled solution. Here, the temperature of the mixed solution is lowered by mixing hot and cold solutions that are pre-saturated with solute.

For efficient mixing, the hot and cold solutions are entered from the non-neighboring inlets of the micromixer to increase the contact area between hot and cold regions and eventually enhance the heat transfer. The equilibrium temperature of the mixed solution is a function of the flow rate and temperature of each stream. This type of cooling also dilutes the concentration of solute in the hot feed and thereby limiting the range of attainable supersaturation in the micromixer.

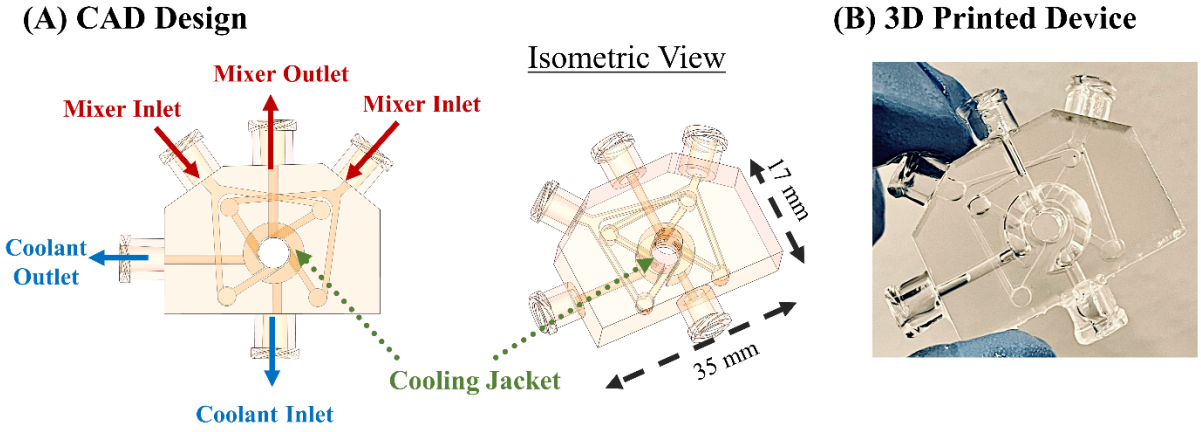

Figure 2: (A) CAD design of the jacketed micromixer. The red directional arrows represent the inlets and outlet of the jacketed microfluidic device; and the blue arrows show the inlet and outlet of the cooling jacket. The green arrow points to the cooling jacket. **(B)** 3D printed jacketed micromixer device.

2.2 Simulation of Temperature, Velocity, Concentration, and Supersaturation Profiles to Evaluate On-the-Spot Quenching Strategies

The effectiveness of above mentioned on-the-spot quenching strategies is evaluated by calculating the temperature and supersaturation profiles in the micromixer.

Convective cooling using external jacket: The dimensions of the micromixers with cooling jackets is provided in section S2.2 of the ESI. The CAD file for design in Figure 2A was imported into COMSOL Multiphysics® and meshed using a free tetrahedral mesh of element size 0.207 to 1.15 mm and a curvature factor of 0.6. The maximum element growth rate and resolution of the narrow regions were set at 1.5 and 0.5, respectively. Navier Stokes equation and the energy balance equation consisting of conduction and convection terms were solved simultaneously for the entering streams of water at different temperatures. The solute was not considered in the simulation as its solubility is typically at least three orders of magnitude smaller than solvent and has a negligible effect on the thermal and viscous properties of the solution. The boundary conditions at the inlets were set according to the entering flow rates and temperature of water in the micromixer and coolant (50 vol% ethylene glycol and water) in the jacket. The boundary condition at the outlet was set to zero conductive flux for the energy balance equation and fixed ambient pressure for the Navier Stokes equation. At the external surface of the device, Newton's law of cooling was applied using the heat transfer coefficient of stagnant air. The details of the simulations are provided in

T_e) of the solution from the mixer was calculated for a range of coolant temperature (T_c), entering solution temperature (T_h), and total volumetric flow rate (Q_t) of solution. A dimensionless temperature (θ) was identified that combines all the temperatures as follows,

$$\theta = \frac{T_e - T_c}{T_h - T_c} \quad (1)$$

Such that θ is only dependent on Q_t. The relationship between θ and Q_t for jacketed microfluidic devices is unique and referred to as a calibration curve, which will be used later to determine the operating conditions of the microfluidic device.

Convective cooling by mixing hot and cold solutions: The dimensions of the micromixer are similar to the case above, except there is no cooling jacket. Here also we used a free tetrahedral mesh of element size 0.207 to 1.15 mm and a curvature factor of 0.6. The maximum element growth rate and resolution of the narrow regions were set at 1.5 and 0.5, respectively. The governing equations and boundary conditions for the simulation of temperature and velocity are similar to the case above. Since the solute concentrations are very low in the solution, the temperature profile was assumed to be independent of the concentration profile. The concentration profile was simulated by solving the Navier Stokes equation and the continuity equation. The boundary conditions at the inlets were set according to the entering flow rates and concentration of solute in the hot and cold streams. The boundary condition at the outlet was set to zero diffusive flux for the continuity equation and fixed ambient pressure for the Navier Stokes equation. The details of the simulations are provided in sections S3.1 and S3.2 of the ESI. The temperature-dependent viscosity and density of the water were also considered in the simulation. The discretized equations were solved using the PARDISO solver, and the residual tolerance was set to 0.01 with 100 iterations and tolerance termination technique. Newton's method was used for iterations with a damping factor of 0.1 and relative tolerance of 0.001. Supersaturation was then calculated using the simulated concentration and temperature profiles. The exit temperature (T_e) of the solution from the mixer was calculated for different values of entering cold solution temperature (T_c), entering hot solution temperature (T_h), and volumetric flow rate (Q_c) of cold solution for a constant total flow rate of 1 mL.min^{-1}. Similar to the first cooling strategy, a dimensionless temperature (θ) was identified (eq. (1)), and a calibration curve of θ vs. Q_c was developed for fixed total flow rate.

3. Materials and Experimental Methods

3.1 Materials

The crystalline β −form of L-glutamic acid (Sigma-Aldrich, chemical purity ≥98%) was used to screen polymorph, morphology, and growth rates during cooling crystallization. The solutions for cooling crystallization studies were made using deionized water (Sigma-Aldrich, 18 MΩ cm). Ethylene glycol was purchased from Sigma Aldrich (Reagent Plus®, ≥99%) and mixed with water (50% vol) was used as the recirculating coolant stream in a jacketed micromixer device.

3.2 Fabrication of the Microfluidic Device

The 3D design of the jacketed micromixer device shown in Figure 2A was designed in SolidWorks® (2020, Dassault Systems) and then 3D printed using a stereolithography (SLA) 3D printer (Form 3, Formlabs Inc., USA). The design has been previously optimized for uniform mixing, trapping of crystals, and compactness.[12,14] A clear FLGPCL02 resin activated by a 405 nm laser was used to 3D print optically clear microfluidic devices with 150 μm of lateral and 25 μm of axial resolutions. The 3D printed devices were washed with isopropyl alcohol (IPA) (90%, Sigma-Aldrich) bath for 20 mins in the Form Wash (Formlabs Inc., USA) to remove the residues of the resin from the external surface. Additionally, the 3D printed supports are loosened after the washing procedure, which helps in their removal post washing. All the interior channels of the 3D printed device and the circulation bath were washed separately by injecting IPA using a syringe to ensure complete removal of the uncured resins. The orientation for prints on the 3D printer stage was selected to minimize the contact of the supports with top and bottom surfaces. However, if necessary, the optical transparency can be improved by wet sanding using 400 to 12000 grit pads followed by spray painting of resin. The top and bottom openings of the micromixers in the multi-inlet device (see Figure 2B) were sealed with polycarbonate films (McMaster-Carr, 0.015 inches) for optical clarity to observe crystals under the optical microscope. The fabricated multi-inlet device is shown in Figure 2B. The details for the fabrication of the jacketed microfluidic device are provided in section S2.3 of the ESI.

3.3 Experimental Setup and Operation of the Cooling Crystallization in the Microfluidic Device

Experimental Setup: The experimental setup for the continuous cooling crystallization of L-glutamic acid involves the multi-inlet micromixer device that is continuously monitored under an optical microscope (Olympus BX53M, Olympus America Inc.) to screen the morphology, polymorph, and growth rate of L-glutamic acid at different supersaturations. The aqueous solution of L-glutamic acid was pumped into the microfluidic device using two single-channel programmed syringe pumps (NE-1000, New Era Pump System Inc.). Two sets of syringe heating pad and heater were used to control the temperature of L-glutamic acid solutions to the desired temperature. Additionally, the heat loss from the syringe heating pads (HEATER-PAD2-1LG New Era Pump System Inc) was measured to calibrate the syringe heater (HEATER-KIT-1LG New Era Pump System Inc), compensate for the heat loss, and finally maintain the temperature of each solution at

the set point. The foam protection wraps were also used to insulate the tubing that connects the syringes to the inlets of the microfluidic device. Both inlets were connected to the one-way microfluidic check valves (LVF-KMM-06, DARWIN Microfluidics) to prevent backflow from the micromixer. A refrigerated recirculation cooling bath (ARCTIC A40, Thermo Fisher Scientific) was used to recirculate a mixture of ethylene glycol and water (50:50 vol ratio) as the coolant stream inside the cooling jacket.

Operation of Jacketed Micromixer: A calibration curve that relates dimensionless exit temperature (θ) with the total volumetric flow rate (Q_t) of the solution was first established computationally and then validated experimentally. The solubility data[10,11] of L-glutamic acid in water along with the calibration curve was used to identify operating conditions to achieve specific supersaturations. For example, to obtain a supersaturation of S=2 at $T_e = 20^\circ\mathrm{C}$, the necessary concentration of entering solution was obtained as follows

$$C = S \times C^* \left(T_e\right) \tag{2}$$

Here C^* is the solubility of L-glutamic acid in water. Next, the total volumetric flow rate was chosen to achieve lower mean residence time and its variance. The total volumetric flow rate Q_t = 1 mL.min^{-1} was chosen that yields a mean residence time of 46.4±27.5 sec (see Figure S7 in section S4 of the ESI). The calibration curve was then used to obtain the value of dimensionless temperature θ for a given Q_t = 1 mL.min^{-1}. From the definition of θ (eq. (1)), the temperature of the entering solution (T_h) was calculated for a choice of coolant temperature (e.g. $T_c = 0^\circ\mathrm{C}$). The supersaturation can be varied by varying the concentration of entering the solution while keeping all other parameters fixed. A total of eight experimental conditions were explored using this cooling strategy. Details of the selected flow rates, feed concentrations, and temperatures are provided in Table S3 in section S5 of the ESI. These operating conditions are also illustrated in Figure S8.

The effective startup of the jacketed microfluidic mixer is crucial for accurate screening of cooling crystallization. The micromixers and channels were first flushed with water to remove air. The coolant stream was then recirculated in the jacket for 15 minutes at a high flow rate of 10 mL.min^{-1} to ensure the device attains an equilibrium temperature. Next, the saturated solutions at temperature T_h are pumped into the micromixer, and the flow rates at both inlets were set equal.

Operation of Non-Jacketed Micromixer that Mixes Hot and Cold Solutions: A calibration curve that relates dimensionless exit temperature (θ

Q_c

$T_e = 40^{\circ}\mathrm{C}$) using eq. (2). Next, we set the flow rate of a cold solution Q_c. The calibration curve (θ vs. Q_c) was then used to obtain the value of θ, which then yields a relation between T_h and T_c (eq. (1)). The entering hot and cold solutions were considered at their saturation limits, such that the concentration of the mixed solution in the mixer is-

$$C = \frac{C_h^* Q_h + C_c^* Q_c}{Q_t} \tag{3}$$

Here C_h^* is the solubility of hot solution at T_h and C_c^* is the solubility of cold solution at T_c. Given the relation between T_h and T_c (eq. (1)), the eq. (3) was then solved to obtain the necessary temperatures of hot and cold solutions. A total of four experimental conditions were explored using this cooling strategy. Details of the selected flow rates, feed concentrations, and temperatures are provided in section S6 of the ESI. These operating conditions are also illustrated in Figure S8.

The effective startup of the hot-and-cold mixing strategy requires flushing the device with water to remove air from the channels and micromixer. Then an aqueous solution of the L-glutamic acid at low temperature is pumped in, and as it fills the micromixer, the high-temperature saturated stream is injected after that.

3.4 Measurements of Growth Rates, Morphology, and Polymorphs

The microscopic images were recorded with a built-in color camera (LC 30, Olympus America Inc.) using transmitted light mode. The time-lapsed images were taken every 60 to 300 seconds to measure growth rates of L-glutamic acid crystals for around 10-30 minutes using OLYMPUS Stream Start software. A longer measurement time was necessary at lower supersaturation.

The time-lapsed images were processed using OLYMPUS Stream Start to measure the growth rate and the percentage of polymorphs of L-glutamic acid crystals. Alternatively, an image analysis program on MATLAB can be used to detect and measure different morphologies of crystals.[15] The polymorphic forms of L-glutamic acid were distinguished based on their distinct morphological forms. The α-form of the L-glutamic crystal is the metastable polymorph and is shaped like a prism, whereas the stable β-form is shaped like needles. The percentage of β-form was calculated based on the fraction of the area covered by the needles.

The prismatic and needle shape morphologies of the α- and β-forms of L-glutamic acid were also confirmed from X-ray diffraction (XRD) spectra obtained using a Bruker D2 PHASER diffractometer with Ni filtered Cu Kα radiation. For all the samples, a step width of 0.2 and a counting time of 5 sec/step were used to enhance the signal-to-noise ratio. Diffraction patterns of L-glutamic acid forms were compared with the literature to confirm the polymorphic form (see section S8 of ESI). [16-19]

4. Results and Discussion

4.1 Temperature Gradient Comparison for the Temperature Control Strategies

Figure 3A shows the steady-state temperature profile in a jacketed microfluidic device. The jacketed device was fed with coolant (50 vol% ethylene glycol in water) at 10 ºC at 10 mL.min^{-1} and the solvent (water) to the micromixer at 70 ºC at 1 mL.min^{-1}. The flow rate of the coolant was high enough to keep the temperature of the jacket uniform. The temperature gradients start developing near the tangential inlets and enter the micromixer, where the solution temperature becomes uniform after 2 mm height from the bottom plan of the cooling jacket. Figure 3B shows the steady-state temperature profile in a microfluidic device without a cooling jacket. This device was fed with hot and cold water through non-neighboring inlets. The cold water at 10 ºC and 0.5 mL.min^{-1} is mixed with hot water at 70 ºC and 0.5 mL.min^{-1}. The total flow rate of water in a micromixer is similar to a jacketed device. However, in this case, the temperature gradient spans a larger height up to 2.75 mm from the bottom plane. This temperature gradient is independent of total flow rate or velocity and is mostly determined by heat diffusion between hot and cold streams.[12] However, the span of the temperature gradient in the jacketed device is mostly determined by the height of the jacket. Figure S5 in the ESI shows the temperature gradients in jacketed and non-jacketed devices.

To compare temperature distributions in Figures 3A and 3B, a thermal homogeneity index is introduced. The thermal homogeneity index at any horizontal plane of the micromixer is defined as:

$$Thermal\ Homogeneity\ Index = 1 - \frac{\sigma^2}{\sigma_0^2}$$

where, σ^2 is the variance of the temperature in any cross-sectional plane and σ_0^2 is the variance of temperature at the bottom plane of the micromixer. Figure 3C shows that for a total flow rate of 1 mL.min^{-1} a slightly lower temperature homogeneity index is observed in the micromixer with hot and cold mixing as compared to the cooling jacket strategy.

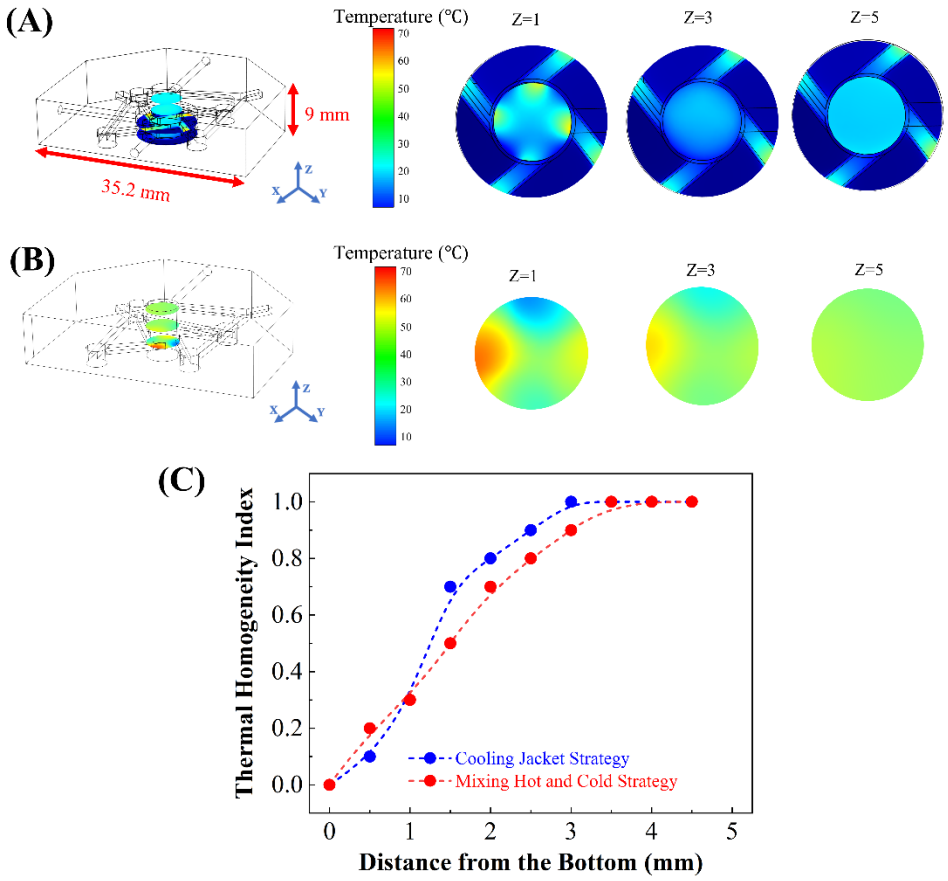

4.2 Attainable Temperatures and Supersaturations in the Micromixer Device

The Navier Stokes equation and the energy balance equation consisting of conduction and convection terms were solved simultaneously to calculate the average temperature of solution exiting micromixer as a function of coolant temperature and temperature and flow rates of inlet streams. These temperatures can be represented collectively as a dimensionless temperature (θ), see eq. (1) , which depends only on the total flow rate (Q_t) of the solution entering the jacketed micromixer. Figure 4A shows an increase in θ with increasing Q_t. The close agreement between experimental and simulation values of θ confirms the accuracy of simulation results. This plot

was used as a calibration curve to determine the necessary flow rate, the temperature of the coolant, and the temperature of the inlet solution to attain the desired temperature in the jacketed-microfluidic device (see details in section 3.3). A desired degree of supersaturation can be achieved by varying saturation concentration or temperature of the inlet solution. The attainable range of supersaturation in such a cooling strategy is therefore determined by the solubility curve.

For the non-jacketed micromixer, the dimensionless temperature depends on the flow rate of hot and cold solutions entering the micromixer. Figure 4B shows a decrease in θ with increasing the flow rate of cold solution for a fixed total flow rate of 1 mL.min^{-1} in the micromixer. A comparison of experimental and simulation values of θ for different temperatures of the cold solution is provided in Figure S6 of the ESI. This plot was used as a calibration curve to determine the necessary flow rate and the temperature of cold and hot solutions to attain the desired temperature in the non-jacketed microfluidic device (see details in section 3.3). For example, θ is 0.5 for 0.5 mL.min^{-1}of the cold saturated stream at 10 ºC, and the equilibrium temperature will be 35 ºC.

The simulation results for suggested temperature control strategies show that the input parameters (T_h, T_c, and Q_t) can be tuned to obtain the desired temperature inside the jacketed microfluidic device. However, in the case of mixing hot and cold solutions, there is a limited range of equilibrium temperature that is feasible over a wide range of input parameters. Figure 4C shows the attainable equilibrium temperature for different values of T_c and Q_c at a fixed total flow rate of 1 mL.min^{-1} and T_h of 70 ºC. Figure 4C is not specific to any compound but is used to calculate the attainable range of the supersaturation for the compound of interest. The accessible range of the supersaturation for the aqueous solution of L-glutamic acid is then obtained using solubility data and equilibrium temperature from Figure 4C. Figure 4D shows that the feasible range of supersaturation for the aqueous solution of L-glutamic acid ranges from 1.03 to 2.03. The highest value of supersaturation is obtained when a saturated cold stream at 10 ºC and a saturated hot stream at 70 ºC are both pumped into the mixer at 0.7 and 0.3 mL.min^{-1}, respectively.

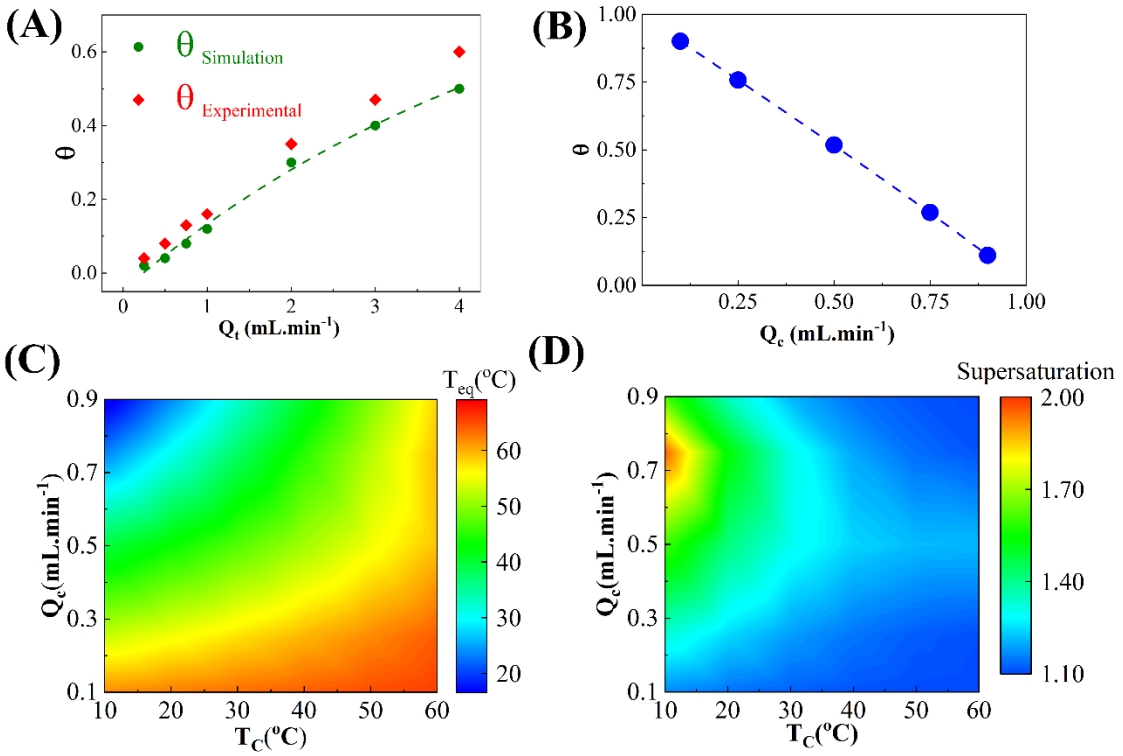

Figure 4: (A) Dimensionless temperature (θ) vs. the total flow rate of the micromixer for the cooling jacket strategy; **(B)** Dimensionless temperature (θ) vs. the flow rate of the saturated cold stream for the hot-and-cold-mixing strategy; **(C)** Equilibrium temperature for the microfluidic mixer in the hot-and-cold-mixing strategy for different flow rate and temperature of the cold stream at fixed T_h and Q_t; **(D)**Accessible range of supersaturation for the cooling crystallization of L-glutamic acid for the hot-and-cold-mixing strategy.

4.3 Screening of Morphology, Polymorphs, and Growth Rate of L-glutamic acid using two Different On-the-Spot Quenching Strategies

The efficacy of the two different on-the-spot quenching strategies – cooling jacket and hot-and-cold mixing – for the microfluidic mixer is evaluated to screen morphology, polymorph, and growth rate of L-glutamic acid via cooling crystallization.

Figures 5A to 5H are the optical images of the L-glutamic acid crystals obtained at different supersaturations using a jacketed microfluidic device. The flow of the recirculating coolant was set to a higher rate of 10 mL.min^{-1} for uniform cooling. At different total flow rates of the L-glutamic acid solution entering the micromixer (1 or 2 mL.min^{-1}), the temperature of the coolant (T_c) and the entering solutions was varied to attain different supersaturations. The temperatures of coolant and saturated L-glutamic acid solutions entering the micromixers A to H are shown in Table 1. The temperature inside the micromixers A to H was obtained from the calibration curve in Figure 4A. The supersaturation in these micromixers is also given in Table 1. The

supersaturation in these eight micromixers decreases in the order of $A > B > C > D > E > F > G > H$. Details for the experimental conditions are provided in section S5 of the ESI. Figures 5A to 5C show the dominant prismatic morphology characteristic of α-form (metastable) of L-glutamic acid. Figure 5D to 5H show an increasing number of the plate and needle-shaped crystals representative of the β-form (stable form).

Figures 5I to 5P show the optical images of the L-glutamic acid crystals obtained at different accessible supersaturations using the hot-and-cold mixing strategy. The total flow rate of hot and cold solution entering the micromixer was set to 1 $ml.min^{-1}$. The temperatures of cold and hot solutions entering the micromixers M to P are given in Table 1. The temperature inside the micromixers M to P was obtained from the calibration curve in Figure 4B. The supersaturation in these micromixers is also given in Table 1. No combination of hot and cold temperatures was identified to achieve supersaturations higher than 1.62, and therefore, Figures 5I to 5L are labeled "Not Accessible." Figure 5M shows a mixture of metastable α-form of prismatic morphology and the stable β-form of the plate-shaped morphology. Figures 5N to 5P show only the stable β-form with the plate and needle-shaped crystals representing the β-form (stable form).

Table 1: Details of Experimental Condition for Cooling Crystallization of the L-glutamic acid.

Samples	T_h (°C)	T_c (°C)	T_{equ} (°C)	Q_{Total} ($mL.min^{-1}$)	$C_{Initial}$ ($mol.\ L^{-1}$)	C_{Mixer} ($mol.\ L^{-1}$)	C_{equ} ($mol.\ L^{-1}$)	Supersaturation
A	50	0	9.30	1	0.152	0.152	0.032	4.78
B	70	10	33.19	2	0.289	0.289	0.076	3.87
C	70	20	39.37	2	0.289	0.289	0.096	3.01
D	60	20	35.39	2	0.214	0.214	0.087	2.45
E	40	20	27.59	2	0.102	0.102	0.059	1.73
F	30	20	23.77	2	0.066	0.066	0.050	1.32
G	50	20	31.46	2	0.091	0.091	0.070	1.29
H	30	0	11.27	2	0.036	0.036	0.033	1.11
M	80	20	50.00	1	0.430	0.239	0.148	1.61
N	70	20	45.00	1	0.290	0.175	0.124	1.42
O	60	20	40.00	1	0.210	0.131	0.101	1.30
P	50	20	35.00	1	0.150	0.098	0.086	1.14

The percentage of stable β-form (X_β) and the growth rates of (111) facet for each condition in Figure 5 were obtained from image analysis using OLYMPUS Stream Start. The α- and β-forms were also confirmed using the XRD (see section S8 of the ESI). Figure 6A shows the variation in X_β as a function of supersaturation in the micromixer. The percentage of the stable form for very low supersaturations ($\sigma \leq 1.3$) is around 100%. It decreases as the supersaturation increases and becomes negligible at higher supersaturations ($\sigma \geq 3$). The percentage of stable form is reported for a steady-state distribution.

The growth rates of L-glutamic acid crystals in micromixers A to P were measured from time-lapsed images taken at a regular time interval for a time period up to 30 minutes. Figure 6B shows the measured growth rates as a function of supersaturation. The equilibrium temperature in micromixers from A to P is labeled next to each data point. The growth rate increases with increasing supersaturations, except for the cases when the temperature is significantly different. The measured growth rates at different supersaturation and temperature compare well with the predicted growth rate.[20,21] The details of growth rate calculations are provided in section S7 of the ESI. The agreement between the measured and predicted growth rates confirms that these on-the-spot quenching strategies are effective approaches to study continuous cooling crystallization using such microfluidic devices.

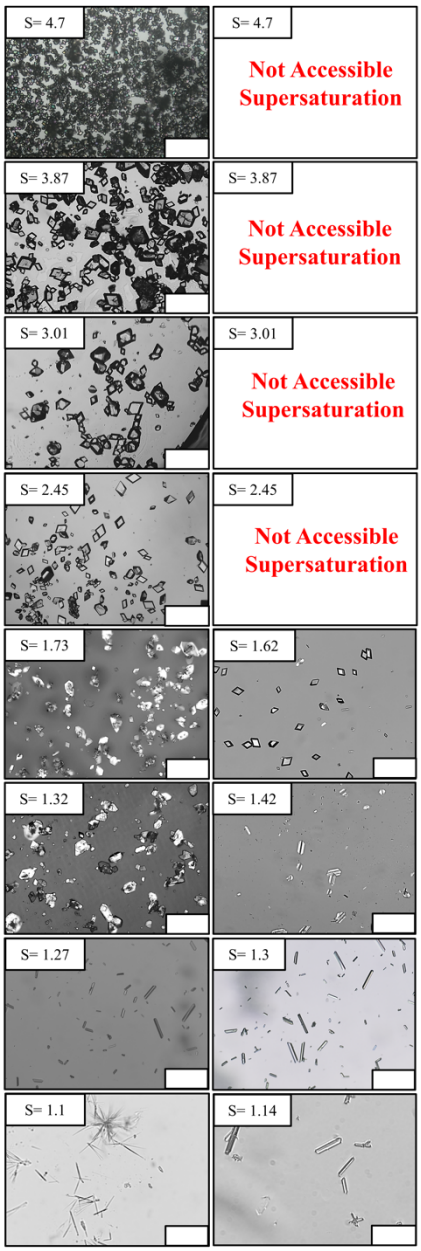

Figure 5: Micrographs of L-glutamic acid crystals obtained at different supersaturations using two different on-the-spot quenching strategies. (The scale bar is 200 μm)

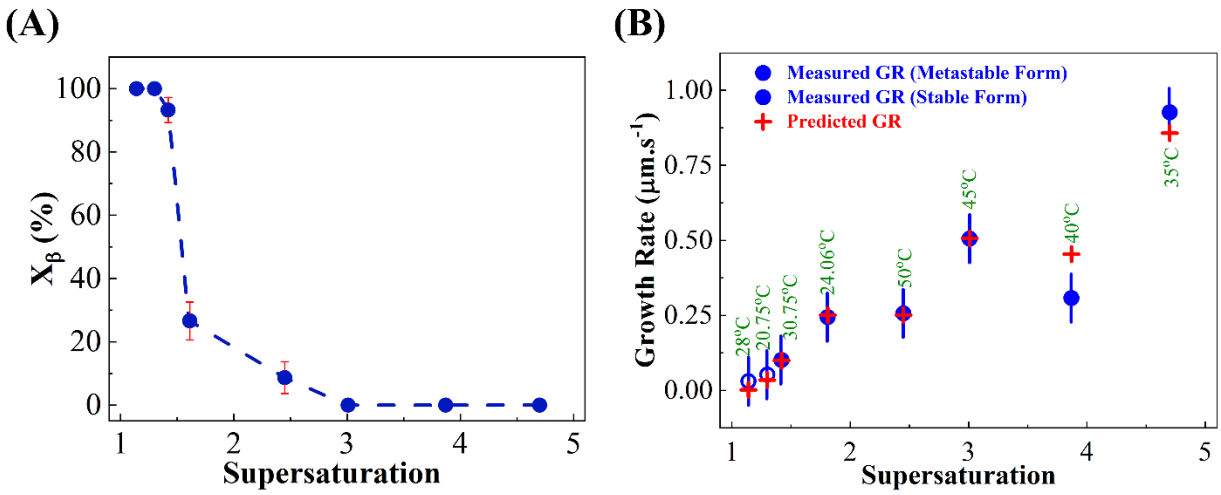

Figure 6: (A) Percentage of the stable polymorph (X_β) of L-glutamic acid at different supersaturation ratios; **(B)** Measured and predicted growth rate (GR) values of the L-glutamic acid crystals at different supersaturation ratios and equilibrium temperatures.

5. Conclusion

Effective implementation of cooling crystallization in a continuous-flow microfluidic device has been challenging primarily due to the development of large temperature gradients and clogging of microchannels. These temperature gradients are dominant near the entrance of the microfluidic channel causing variations in supersaturation. Additionally, the depletion of supersaturation due to crystal nucleation and growth in the channel has prevented the successful evaluation of cooling crystallization in a continuous-flow microfluidic device. Here, two effective strategies to reduce temperature gradients in the microfluidic device are presented that involve on-the-spot quenching of entering solutions for continuous cooling crystallization at constant supersaturation. The first strategy involves a collar of the cooling jacket around the micromixer, and the second strategy utilizes the mixing of a hot and cold solution. The temperature gradients in the jacketed-microfluidic device are determined by the height of the jacket, which can be smaller than 1 mm, whereas the temperature gradients in the second strategy are governed by the mixing efficiency of a hot and cold solution. The cooling jacket allows access to a full range of supersaturations based on the solubility curve. However, the attainable supersaturations in the hot-and-cold-mixing strategy are significantly limited by the temperature and concentration difference between hot and cold streams. Based on these attributes of two different temperature control strategies, the cooling jacket strategy is better suited to study higher supersaturations, and the hot-and-cold-mixing strategy is preferred for targeting the lower range of supersaturations.

Here we demonstrate comparative screening of crystal morphology, polymorph, and growth rates of L-glutamic acid for eight different conditions employing both on-the-spot

quenching approaches. The cyclonic flow in the micromixer allows the trapping of crystals and helps in attaining homogeneous temperature. The compact design of the jacketed and non-jacketed microfluidic device permits direct placement of the device under an optical microscope to take time-lapse images for measurement of morphology, polymorph, and growth rate. The maximum supersaturation attained is 4.7 in the cooling jacket strategy, whereas the hot-and-cold-mixing strategy could only screen supersaturations up to 1.6. Both cooling strategies are effective in measuring growth rates of L-glutamic acid crystals at given supersaturations and temperatures, which is in good agreement with the predicted values. These strategies also show a similar trend in the decrease of β-form of L-glutamic acid crystals with increasing supersaturation.

This article presents design rules to implement on-the-spot quenching in a continuous-flow microfluidic device and thereby provides a solution to one of the major challenges in studying cooling crystallization in such systems. The kinetic and polymorphic data obtained from such devices can help in scale up of crystallizers. In addition to these advantages, these devices can be modified to screen protein crystals. We expect these on-the-spot quenching strategies will have a transformative impact on the continuous-flow microfluidics for various healthcare and energy applications.

Disclosure

Data were generated by the University of Illinois at Chicago. AbbVie Inc., North Chicago, USA, provided experimental support for a summer internship of Paria Coliaie. Dr. Manish S. Kelkar, Dr. Akshay Korde, and Dr. Nandkishor K. Nere are present employees of AbbVie Inc.

Conflicts of Interest

A PCT application (PCT/US20/36353) titled “Continuous-Flow, Well Mixed, Microfluidic Crystallization Device for Screening Polymorphs, Morphologies and Crystallization Kinetics at Controlled Supersaturation,” has been filed.

Acknowledgement

This material is based on the work performed in the Materials and Systems Engineering Laboratory at the University of Illinois at Chicago in collaboration with Enabling Technology Consortium (ETC: https://www.etconsortium.org/, specifically AbbVie, Biogen, Bristol Myers Squibb, and Takeda Pharmaceuticals). P.C. and M.R.S. acknowledge funding support from ETC to conduct this work. P.C. acknowledges the summer internship opportunity at AbbVie Inc. to conduct a few experiments for the completion of this work. The authors also thank Moussa Boukerche, Jie Chen, Daniel Pohlman, Bradley Greiner, Pankaj Shah, and Kushal Sinha for their comments and suggestions. The authors would also like to acknowledge the leadership support from Samrat Mukherjee, Ahmad Sheikh, and Shailendra Bordawekar of AbbVie Inc.

References

(1) Mersmann, A.: *Crystallization technology handbook*; CRC press, 2001.

(2) Nagy, Z. K.; Braatz, R. D.: Advances and new directions in crystallization control. *Annual review of chemical and biomolecular engineering* **2012**, *3*, 55-75.

(3) Miralles, V.; Huerre, A.; Malloggi, F.; Jullien, M.-C.: A review of heating and temperature control in microfluidic systems: techniques and applications. *Diagnostics* **2013**, *3*, 33-67.

(4) Singh, M.; Nere, N.; Tung, H. H.; Mukherjee, S.; Bordawekar, S.; Ramkrishna, D.: Measurement of Polar Plots of Crystal Dissolution Rates using Hot-Stage Microscopy. Some Further Insights on Dissolution Morphologies. *Under Review in Crystal Growth & Design* **2014**.

(5) Galkin, O.; Vekilov, P. G.: Direct determination of the nucleation rates of protein crystals. *The Journal of Physical Chemistry B* **1999**, *103*, 10965-10971.

(6) Gong, T.; Shen, J.; Hu, Z.; Marquez, M.; Cheng, Z.: Nucleation rate measurement of colloidal crystallization using microfluidic emulsion droplets. *Langmuir* **2007**, *23*, 2919-2923.

(7) Yang, J.; Liu, Y.; Rauch, C. B.; Stevens, R. L.; Liu, R. H.; Lenigk, R.; Grodzinski, P.: High sensitivity PCR assay in plastic micro reactors. *Lab on a Chip* **2002**, *2*, 179-187.

(8) Guijt, R. M.; Dodge, A.; van Dedem, G. W.; de Rooij, N. F.; Verpoorte, E.: Chemical and physical processes for integrated temperature control in microfluidic devices. *Lab on a Chip* **2003**, *3*, 1-4.

(9) Maltezos, G.; Rajagopal, A.; Scherer, A.: Evaporative cooling in microfluidic channels. *Applied physics letters* **2006**, *89*, 074107.

(10) Jiang, M.; Zhu, Z.; Jimenez, E.; Papageorgiou, C. D.; Waetzig, J.; Hardy, A.; Langston, M.; Braatz, R. D.: Continuous-flow tubular crystallization in slugs spontaneously induced by hydrodynamics. *Crystal growth & design* **2014**, *14*, 851-860.

(11) Kim, S.; Kim, H. J.; Jeon, N. L.: Biological applications of microfluidic gradient devices. *Integrative Biology* **2010**, *2*, 584-603.

(12) Coliaie, P.; Kelkar, M. S.; Nere, N. K.; Singh, M. R.: Continuous-flow, well-mixed, microfluidic crystallization device for screening of polymorphs, morphology, and crystallization kinetics at controlled supersaturation. *Lab on a Chip* **2019**, *19*, 2373-2382.

(13) Coliaie, P.; Kelkar, M. S.; Langston, M.; Liu, C.; Nazemifard, N.; Patience, D.; Skliar, D.; Nandkishor, N.; Singh, M. R.: Advanced Continuous-Flow Microfluidic Device for Parallel Screening of Crystal Polymorphs, Morphology and Kinetics at Controlled Supersaturation. *Lab on a Chip* **2021**.

(14) Coliaie, P.; Kelkar, M. S.; Langston, M.; Liu, C.; Nazemifard, N.; Patience, D.; Skliar, D.; Nere, N. K.; Singh, M. R.: Advanced continuous-flow microfluidic device for parallel screening of crystal polymorphs, morphology, and kinetics at controlled supersaturation. *Lab on a Chip* **2021**.

(15) Singh, M. R.; Chakraborty, J.; Nere, N.; Tung, H. H.; Bordawekar, S.; Ramkrishna, D.: Image-Analysis-Based Method for 3D Crystal Morphology Measurement and Polymorph Identification Using Confocal Microscopy. *Crystal Growth & Design* **2012**, *12*, 3735-3748.

(16) Hirayama, N.; Shirahata, K.; Ohashi, Y.; Sasada, Y.: Structure of α Form of L-Glutamic Acid. α-β Transition. *Bulletin of the Chemical Society of Japan* **1980**, *53*, 30-35.

(17) Wantha, L.; Punmalee, N.; Sawaddiphol, V.; Flood, A. E.: Effect of Ethanol on Crystallization of the Polymorphs of L-Histidine. *Journal of Crystal Growth* **2018**, *490*, 65-70.

(18) Lehmann, M. S.; Koetzle, T. F.; Hamilton, W. C.: Precision neutron diffraction structure determination of protein and nucleic acid components. VIII: the crystal and molecular

structure of the β-form of the amino acid l-glutamic acid. *Journal of Crystal and Molecular Structure* **1972**, *2*, 225-233.

(19) Ruggiero, M. T.; Sibik, J.; Zeitler, J. A.; Korter, T. M.: Examination of l-Glutamic Acid Polymorphs by Solid-State Density Functional Theory and Terahertz Spectroscopy. *The Journal of Physical Chemistry A* **2016**, *120*, 7490-7495.

(20) Schöll, J.; Lindenberg, C.; Vicum, L.; Brozio, J.; Mazzotti, M.: Precipitation of α L-glutamic acid: determination of growth kinetics. *Faraday Discussions* **2007**, *136*, 247-264.

(21) Dighe, A. V.; Singh, M. R.: Solvent fluctuations in the solvation shell determine the activation barrier for crystal growth rates. *Proceedings of the National Academy of Sciences* **2019**, *116*, 23954-23959.